Redox cycling amplified electrochemical detection of DNA hybridization: Application to pathogen *E. coli* bacterial RNA

Anne Walter [a,c], Jie Wu [a,b,*], Gerd-Uwe Flechsig [c], David A. Haake [d,e], Joseph Wang [a,**]

[a] *Department of Nanoengineering, University of California San Diego, La Jolla, CA 92093, United States*
[b] *Key Laboratory of Analytical Chemistry for Life Science (Ministry of Education of China), Department of Chemistry, Nanjing University, Nanjing 210093, PR China*
[c] *University of Rostock, Department of Chemistry, Dr.-Lorenz-Weg 1, D-18051 Rostock, Germany*
[d] *Department of Medicine, David Geffen School of Medicine at University of California Los Angeles, Los Angeles, CA 90095, United States*
[e] *Veterans Affairs Greater Los Angeles Healthcare System, Los Angeles, CA 90073, United States*

ARTICLE INFO

ABSTRACT

An electrochemical genosensor in which signal amplification is achieved using *p*-aminophenol (*p*-AP) redox cycling by nicotinamide adenine dinucleotide (NADH) is presented. An immobilized thiolated capture probe is combined with a sandwich-type hybridization assay, using biotin as a tracer in the detection probe, and streptavidin-alkaline phosphatase as reporter enzyme. The phosphatase liberates the electrochemical mediator *p*-AP from its electrically inactive phosphate derivative. This generated *p*-AP is electrooxidized at an Au electrode modified self-assembled monolayer to *p*-quinone imine (*p*-QI). In the presence of NADH, *p*-QI is reduced back to *p*-AP, which can be re-oxidized on the electrode and produce amplified signal. A detection limit of 1 pM DNA target is offered by this simple one-electrode, one-enzyme format redox cycling strategy. The redox cycling design is applied successfully to the monitoring of the 16S rRNA of *E. coli* pathogenic bacteria, and provides a detection limit of 250 CFU μL^{-1}.

© 2011 Elsevier B.V. All rights reserved.

1. Introduction

In recent years, researchers have been challenged to push the sensitivity of electrochemical DNA sensor down to subnanomolar levels while keeping these procedures as simple, reliable, and cost-effective as possible. Signal amplification is the most important strategy in lowering the detection limits [1,2]. In particular, most of the signal-amplification methods have been developed by employing different labels, such as functionalized liposomes [3,4], multiple enzyme coated microsphere [5] or carbon nanotube [6], bio-barcode Au nanoparticals [7], arrays of Au [8] and CdS nanoparticles [9], and dendritic-like enzyme nanoarchitectures [10]. During these labels, enzymes are still the most commonly used ones for signal amplification due to their high turnover frequencies and high reaction selectivity.

Alkaline phosphatase (ALP) is one of the most used enzymatic labels for the DNA hybridization assay. For the measurement of ALP,

a standard method is that ALP dephosphorylates *p*-aminophenyl phosphate (*p*-APP) enzymatically to produce electroactive species *p*-aminophenol (*p*-AP), which is detected amperometrically by substrate electrode. This approach has been widely used in the electrochemical enzyme immunoassays [11,12], as well as DNA hybridizations [13]. However, ALP detection suffers from drawbacks ultimately related to the limited stability of *p*-APP and *p*-AP. Substrate redox cycling, which is related to the regeneration of enzyme-amplified electroactive species after their oxidation or reduction, is a well-suited means to overcome this defect [14]. Furthermore, since the redox reaction of the regenerated species provides an enhanced electrochemical signal, higher signal amplification could be achieved by the combination of enzymatic amplification with a substrate redox cycling step [15–17].

Generally, redox cycling can be achieved electrochemically [18,19], enzymatically [20–23], or chemically [15,24–26]. In the model of electrochemical redox cycling, the electroactive species oxidized at one electrode are reduced back at the second electrode, so two working electrodes or an interdigitated array electrode are needed, while it conflicts with the requirement of simpleness and cost-effectiveness for DNA sensor. Enzymatic redox cycling provides a relatively simple way for redox cycling amplification [14,20,23]. However, in this model multiple enzymes are required and the redox cycling efficiency is highly dependent on the enzyme kinetics.

* Corresponding author at: Key Laboratory of Analytical Chemistry for Life Science (Ministry of Education of China), Department of Chemistry, Nanjing University, Nanjing 210093, PR China. Tel.: +86 258 359 3593; fax: +86 258 359 3593.
** Corresponding author. Fax: +1 858 534 9553.
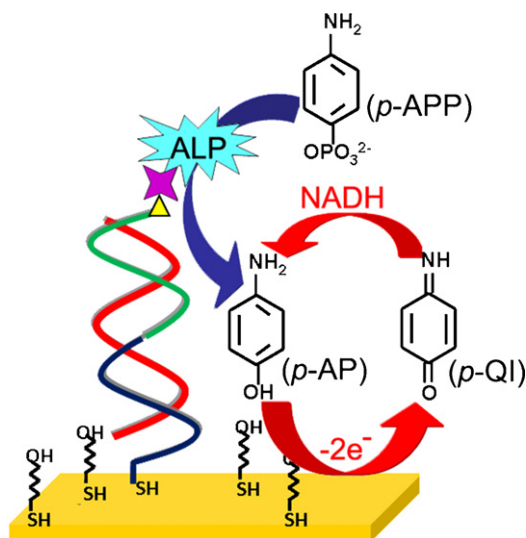*E-mail addresses:* wujie@nju.edu.cn (J. Wu), josephwang@ucsd.edu (J. Wang).

Fig. 1. Schematic illustration of DNA sensor using p-AP redox cycling by NADH on Au substrate.

Recently, a new upsurge in chemical redox cycling is in the making. Hydrazine and sodium borohydride were reported to use in p-AP redox cycling and shown good performance in immunosensor. In order to get lower background currents in electrochemical detection, the use of strong reducing agents, such as hydrazine and sodium borohydride, which are easily oxidized electrochemically at low potentials, is limited on highly electrocatalytic metal electrodes, for example, Au electrode. Benefit from both the slow electrochemical oxidation on metal electrodes and fast chemical reaction, nicotinamide adenine dinucleotide (NADH) is a good substitute for strong reducing agents in redox cycling system on metal electrodes [16].

16S rRNA gene, which is universal in bacteria, is normally used for bacterial identification and phylogenetic studies due to its variable and conserved regions [27]. The goal of the present work is to design an amplified electrochemical genosensor for sensitive sensing of 16S rRNA gene with chemical redox cycling using NADH. In this approach, the cycling was applied to an electrochemical DNA sensor based on Au working electrodes. Following a sandwich-type hybridization assay, ALP enzymes are conjugated to the surface of the genosensor, and enzymatically generate the electroactive mediator p-AP from p-APP (Fig. 1). The produced p-AP is then electrooxidized at the Au working electrode to p-quinone imine (p-QI). Immediately p-QI is reduced back to p-AP by NADH, which leads to the redox cycling of the p-AP to amplify the electrical current. Such procedure provides good performance for DNA detection as well as sensitive measurements of the pathogen $E.$ $coli$ bacteria.

2. Experimental

2.1. Reagents

6-Mercapto-1-hexanol (MCH), Trizma hydrochloride (Tris–HCl), ethylenediaminetetraacetic acid, sodium chloride, sodium hydroxide, sodium phosphate monobasic, sodium phosphate dibasic, potassium chloride, potassium phosphate dibasic, potassium phosphate monobasic, bovine serum albumin, streptavidin-alkaline phosphatase (SA-ALP), p-AP, and NADH were purchased from Sigma-Aldrich (St. Louis, MO). The blocking agent casein was obtained from Pierce (Rockford). p-APP was purchased from Biosynth International Inc. (Switzerland). Magnesium sulfate was received from EMD Chemicals Inc.

The buffer solutions used in this study were as follows: The DNA immobilization buffer (IB) was 10 mM Tris–HCl, 1 mM ethylenediaminetetraacetic acid, and 0.3 M NaCl (pH 8.0). The hybridization buffer (HB) was a 1 M phosphate buffer solution containing 0.78 M K_2HPO_4, 0.27 M NaH_2PO_4 and 2.5% bovine serum albumin (pH 7.2). The binding buffer (BB) for associating with SA-ALP consisted of 0.14 M NaCl, 0.003 M KCl, 0.002 M KH_2PO_4, 0.01 M Na_2HPO_4 and 0.5% casein (pH 7.2). The buffer for electrochemical experiments (EB) consisted of 50 mM Tris, 10 mM KCl, and 1 g L^{-1} $MgCl_2$ (pH 9.0). Solutions of p-AP and p-APP were prepared daily in the EB.

All synthetic oligonucleotides were purchased from Thermo Fisher Scientific (Ulm, Germany). The sequences of the thiolated capture probe, biotinylated detection probe, complementary target, non-complementary target and single-base mismatched (SBM) target are 5′-Thiol-TAT TAA CTT TAC TCC-3′, 5′-CTT CCT CCC CGC TGA-Biotin-3′, 5′-TCA GCG GGG AGG AAG GGA GTA AAG TTA ATA-3′, 5′-CTG GGG TGA AGT CGT AAC AAG GTA ACC GTA GGG GAA C-3′ and 5′-TCA GCG GGG AGG AAG GGA GTA AAA TTA ATA-3′, respectively. The specific region of $E.$ $coli$ 16S rRNA gene for the capture probe is positions from 447 to 461 according to the 5′ → 3′ nucleotide sequence. The $E.$ $coli$ pathogen isolates were obtained from the University of California-Los Angeles (UCLA) medicine department. One milliliter of bacteria in Luria broth (containing 4.5×10^7 CFU, estimated from optical density measurements at 600 nm) was centrifuged at $10,000 \times g$ for 5 min. The supernatant was discarded, and the bacteria left in the centrifuge tube were stored at $-80\,^\circ$C to prepare the bacterial isolate pellets.

2.2. Apparatus

Voltammetry and chronoamperometry were performed using a PalmSens hand-held potentiostat equipped with an 8-channel PalmSens Multiplexer (CH8) (Palm Instruments BV, Electrochemical Sensor Interfaces, Netherlands). All the experiments were performed on the 16-sensor array, in which each sensor consisted of a central Au working electrode surrounded by an Au reference and an Au auxiliary electrode.

2.3. Genosensor's fabrication

DNA hybridization was performed on an array of 16 gold electrodes (2.5 mm diam.; GeneFluidics Inc., Monterey Park, CA). The Au electrodes were incubated with a 6-μL aliquot of the 0.5 μM thiolated capture probe in the IB overnight at 4 $^\circ$C in a humidified surrounding. Subsequently, the electrode array was washed with deionized water and dried with nitrogen. After this, the probe-modified Au electrodes were treated with 6 μL of the 1 mM MCH in IB for 50 min to obtain a mixed self-assembled monolayer (SAM). Finally, the sensors were thoroughly rinsed with water and dried under nitrogen.

2.4. DNA hybridization assay

The DNA detection strategy is based on a sandwich-type hybridization assay. Different concentrations of the DNA target were mixed with the biotinylated detection probe (0.25 μM) in the HB. Aliquots (4 μL) of this target/detection-probe hybrid solution were cast on each of the oligonucleotide-modified gold sensors and were incubated for 15 min. After the sensors were washed and dried, a 4-μL aliquot of 2.33 U mL^{-1} SA-ALP (in the BB) was cast on each sensor and was incubated for 15 min to allow the enzyme binding, followed by washing with water and drying with nitrogen. A 50 μL EB containing a mixture of 2 mM p-APP and 2 mM NADH was subsequently dropped on each sensor and the enzymatic reaction proceeded for 30 min (under dark). Finally, the bioelectrocatalytic detection of the p-AP was carried out chronoam-
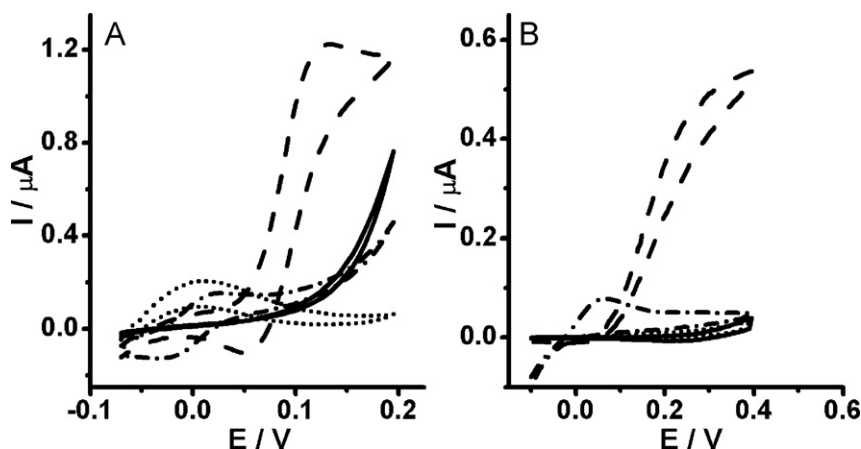
Fig. 2. Cyclic voltammograms of bare Au electrode (A) and SAM-modified Au electrode (B) in EB (solid line), containing 5 mM (A) or 2 mM (B) NADH (dotted line), 0.5 mM (A) or 0.1 mM (B) *p*-AP (dashed dotted line) and both 5 mM NADH and 0.5 mM *p*-AP (A) or both 2 mM NADH and 0.1 mM *p*-AP (B) (dashed line) at a scan rate of 5 mV s^{-1}.

perometrically using the chemical recycling electrode system at +0.3 V.

2.5. E. coli 16S rRNA hybridization assay

The applicability of the present method was tested with genetic material (16S rRNA) corresponding to *E. coli* pathogenic bacteria. To produce the *E. coli* 16S rRNA, the bacteria were lysed by resuspending a pellet containing 4.5×10^7 CFU bacteria (as determined by serial plating) in 10 μL of 1 M NaOH and waiting for 5 min. A 50-μL aliquot of the biotinylated detection-probe (0.25 μM) in HB was added to the 10 μL bacterial lysate, leading to genetic material with a concentration of 4.5×10^7 CFU per 60 μL. This solution was serially diluted in the 0.25 μM biotinylated detection probe solution to provide different concentrations of the bacterial genetic material (16S rRNA). A 10-min incubation was used for hybridizing the detection probe to the target. Aliquots (4 μL) of this bacterial-target/detection-probe hybrid were cast on each capture-probe modified sensor and incubated for 15 min, followed by capture of the ALP enzyme. The enzymatic reaction and electrochemical detection steps are described earlier for the DNA hybridization assay. All procedures were carried out at room temperature.

3. Results and discussion

3.1. p-AP redox cycling by NADH

Redox cycling of *p*-AP by NADH and its use in electrochemical immunoassay has been pioneered by Kwak et al. [16]. Different from other chemical redox cycling, this system is unique in the use of metal working electrodes. However, a ferrocenyl-tethered dendrimer layer was required for electrode modification to fast the electron transfer rate. In order to investigate the redox cycling phenomenon of *p*-AP directly on Au electrode without extra mediator layer, we obtained the cyclic voltammograms of NADH and *p*-AP or their mixture on bare (Fig. 2A) and SAM modified Au electrodes (Fig. 2B), respectively.

A pair of reversible peaks of *p*-AP were observed with a redox potential of +0.025 V on bare Au surface (Fig. 2A, dashed dotted line). In the presence of NADH, the shape of the voltammogram changed to a catalytic sigmoidal curve. The oxidation (anodic) current of *p*-AP was enhanced as the reduction (cathodic) current decreased (Fig. 2A, dashed line), which can be ascribed to the electrochemical oxidation of *p*-AP to *p*-QI coupled with the NADH reduction of *p*-QI back to *p*-AP. However, the anodic current of NADH on bare Au electrode was considerable (Fig. 2A, dotted line),

and was not sufficient to obtain low background currents. When the Au electrode was modified with a SAM of thiol molecule, the anodic current of NADH decreased significantly (Fig. 2B, dotted line), which makes it possible to apply NADH redox cycling on Au subtrate electrode. Because the insulating SAM may cause slow electron transfer between the electrode and electroactive species, only an irreversible anodic peak of *p*-AP can be observed (Fig. 2B, dashed dotted line). However, a similar redox cycling response to that on bare Au surface was obtained on the SAM modified Au. Upon the addition of NADH to *p*-AP solution, a greatly enhanced electrochemical response with a sigmoidal shape in the voltammogram was observed (Fig. 2B, dashed line), which means it's possible to apply *p*-AP/NADH redox cycling on SAM modified Au electrode, but without mediator layer.

3.2. Stability of p-AP

p-APP has been widely used as a substrate of ALP, because the enzymatic product *p*-AP could be measured amperometrically at a low potential [28,29]. Nevertheless, it is well known that *p*-AP is not stable; it can be easily oxidized by air and is light-sensitive. Thus, the time of enzyme reaction for accumulation of the product was limited, which lowered the sensitivity and reproducibility in detection of ALP. Recently, redox cycling using reducing agents, such as hydrazine, is suggested for prevention the aerial oxidation of *p*-AP, enabling longer incubation time [15]. Here, the stability of the electrochemical responses of *p*-AP with and without NADH, the reducing agent for *p*-AP redox cycling used in this study, is examined (Fig. 3). *p*-AP (0.1 mM) and the mixture solution of *p*-AP (0.1 mM) and NADH (2 mM) were detected voltammetrically every 30 min after freshly preparation, and over a period of 120 min. The plot of voltammetric response *vs* time indicates that the electrochemical signal of *p*-AP decreased 84% after 2 h, in contrast, signal of *p*-AP in the presence of NADH is stable with a gentle increase, showing that the use of NADH in detection solution could prevent the aerial oxidation of *p*-AP and enable a longer incubation time.

3.3. p-AP/NADH redox cycling based electrochemical hybridization assay

The schematic diagram of DNA sensor using *p*-AP redox cycling by NADH on Au substrate was illustrated in Fig. 1. Hybridization of the surface-confined capture probe with the target/biotinylated-detection-probe conjugate results in a sandwich structure on the modified gold surface. Through a streptavidin-biotin conjugation ALP was bound to this biotinylated sandwich complex, and the
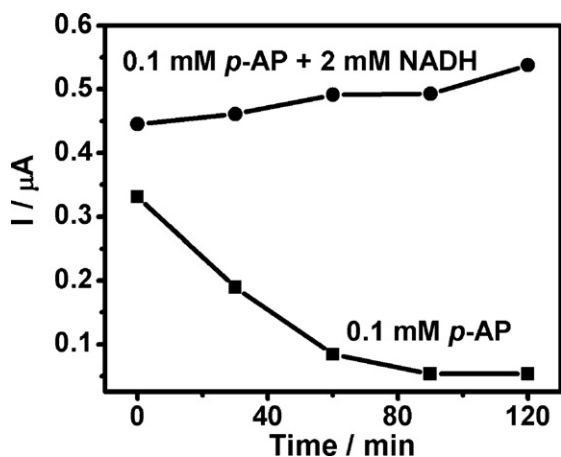
Fig. 3. Chronoamperometric response of SAM-modified Au electrodes in DB containing 0.1 mM p-AP and both 0.1 mM p-AP and 2 mM NADH at +0.3 V with different interval times (0, 30, 60, 90, 120 min) after the preparation of the p-AP solution.

Fig. 4. Cyclic voltammograms of 0 nM DNA (curves a and b) and 10 nM DNA (curves c and d) in EB containing 2 mM p-APP (curves b and c) and both 2 mM p-APP and 2 mM NADH (curves a and d) at a scan rate of 5 mV s^{-1}.

amount of bound ALP is proportional to the concentration of target DNA. After addition of substrate p-APP the enzymatic reaction from p-APP to p-AP proceeded, this was continued for 30 min, followed by the electrochemical detection of the generated p-AP. In the presence of NADH p-AP can be cycled after its electro-oxidization on the electrode, enabling the increase of the anodic current. Fig. 4 shows the cyclic voltammograms of DNA sensor in the substrate solution with (Fig. 4, curve a and d) and without NADH (Fig. 4, curve b and c). Without NADH, the response for DNA target can be only from the electro-oxidization of enzymatic generated p-AP (Fig. 4, curve c). Upon the addition of NADH, the anodic current for DNA target with the same concentration was greatly enhanced (Fig. 4, curve d), showing signal amplification by redox cycling.

The analytical performance of the DNA hybridization using p-AP/NADH redox cycling was characterized under the optimal experimental conditions and using microliter (4 μL) samples. Fig. 5A displayed the chronoamperometric responses obtained at +0.3 V for different concentrations of the DNA target: (a) 0 nM, (b) 1 pM, (c) 10 pM, (d) 100 pM, (e) 1 nM, (f) 10 nM, (g) 100 nM. The resulting calibration plot, shown in Fig. 5B, indicates a nonlinear logarithmic function between the chronoamperometric signal and the target DNA concentration, spanning an impressive response region of 5 orders of magnitude. Comparing with the previous study using nanocatalyst-based substrate redox cycling [25] strat-
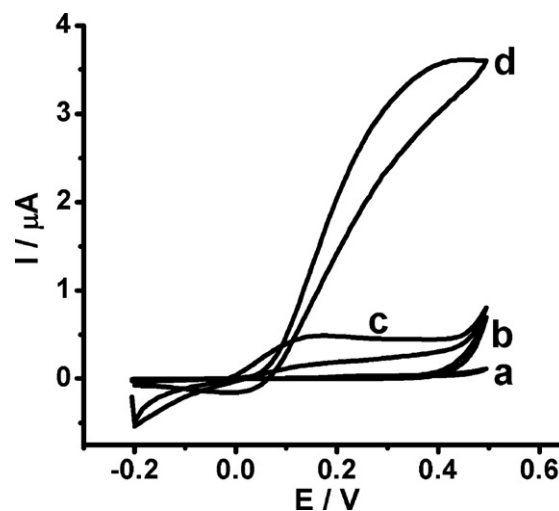
egy, the proposed method offered a ~10 times higher sensitivity. A detection limit of 1 pM DNA can thus be explored by the proposed method, which corresponds to 4 amole in the 4 μL sample. This detection limit was 100-fold better than that of a previously report without NADH [13]. The selectivity of the present assay was tested by challenging the system with non-complementary and SBM oligonucleotides. As shown in Fig. 6, the response for 100 nM non-complementary DNA (curve b) is higher than that for the control (curve a), but it is still clearly smaller than that from 1 pM target DNA (curve c), which is 1×10^5 times lower than the concentration of non-complementary DNA. However, the signal of 1 nM SBM DNA is 81.2% of that of complementary target with the same concentration, which might be that the hybridization free energy between complementary and SBM DNA target to the probe is close due to the relative long sequence of the target DNA (30 bases with 46.7% GC content) [30]. Further discrimination against closely mismatched oligonucleotides could be achieved using stringent control of the hybridization and washing conditions or using specific peptide nucleic acid probes.

The real-life utility of the DNA hybridization assay using p-AP/NADH redox cycling was illustrated for the detection of 16S rRNA of E. coli pathogenic bacteria. Fig. 7 displays the chronoam-
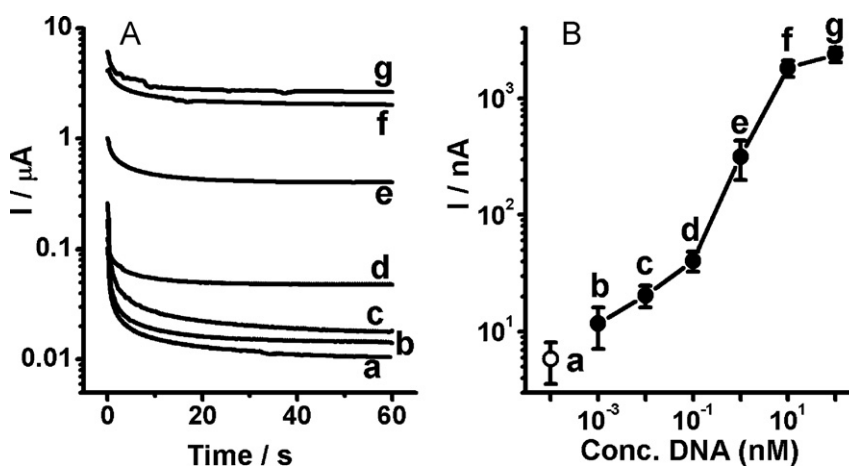

Fig. 5. Chronoamperometric response (A) at +0.3 V and calibration plot (B) for different concentrations of the DNA target: (a) 0 nM, (b) 1 pM, (c) 10 pM, (d) 100 pM, (e) 1 nM, (f) 10 nM, and (g) 100 nM. Error bars represent the standard deviation of six parallel experiments. NADH concentration, 2 mM.
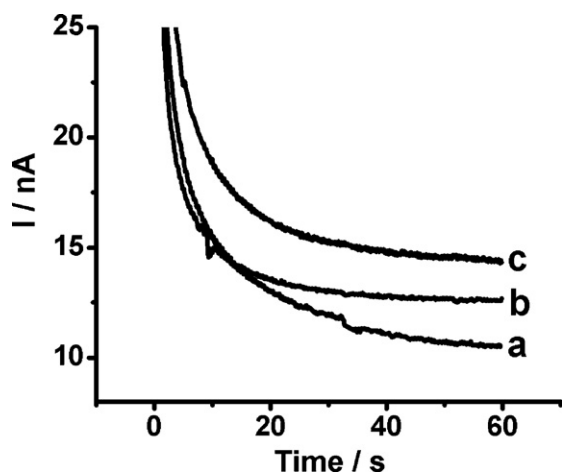
Fig. 6. Chronoamperometric responses at +0.3 V to (a) 0 nM target DNA, (b) 100 nM non-complementary DNA and (c) 1 pM target DNA.

perometric responses obtained for samples containing increasing levels of the pathogen *E. coli* bacteria (a) 0, (b) 38, (c) 960, (d) 4.8×10^3, (e) 2.4×10^4, (f) 1.2×10^5, and (g) 6×10^5 CFU per sensor. The calibration plot indicates a nonlinear logarithmic function between the chronoamperometric signals and the levels of the pathogen *E. coli* bacteria down to 960 CFU per sensor. Considering the $4\,\mu L$ sample volume such detection limit corresponds to $250\,CFU\,\mu L^{-1}$. *E. coli* contains between 5×10^3 and 2×10^4 copies of 16S rRNA per cell [31]. Therefore, the present detection limit of $250\,CFU\,\mu L^{-1}$ can be translated to the detection of ribosome copies from 2 to 10 pM, which compares favorably with the detection limit of DNA target described in Fig. 5.

The reproducibility of the proposed method was evaluated by five parallel measurements using five different chips. Relative standard deviations of 18.7% and 6.4% were obtained for 100 pM target DNA and 16S rRNA corresponding to 4.8×10^3 CFU per sensor, respectively, indicating acceptable fabrication reproducibility.
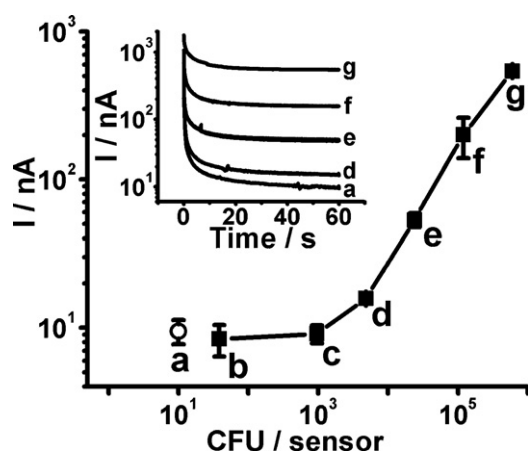

Fig. 7. Calibration plot for different concentrations of the pathogen *E. coli* bacteria (a) 0, (b) 38, (c) 960, (d) 4.8×10^3, (e) 2.4×10^4, (f) 1.2×10^5, and (g) 6×10^5 CFU per sensor. Error bars represent the standard deviation of six parallel experiments. Insert figure: relating chronoamperometric response for calibration plot of the pathogen *E. coli*.

4. Conclusions

We have described a DNA electrochemical sensor based on signal amplification by both enzymatic amplification and substrate redox cycling. The redox cycling is achieved simply by adding a reducing agent, NADH, to the detection solution, and could be applied to an electrochemical DNA sensor based on Au working electrodes. Electroactive product, *p*-AP, is well protected from oxidation by air in the presence of reducing regent, a long enzymatic accumulation time is possible in thus chemical redox cycling system, which could further reduce the detection limit. The convenient use of DNA biosensor arrays in association with a simple one-electrode, one-enzyme format redox cycling strategy led to the specific and sensitive detection of 1 pM DNA target, as well as $250\,CFU\,\mu L^{-1}$ *E. coli* pathogenic bacteria, which shows great potential in clinical application.

References

[1] N.L. Rosi, C.A. Mirkin, Chem. Rev. 105 (2005) 1547–1562.
[2] J. Wang, Small 1 (2005) 1036–1043.
[3] F. Patolsky, A. Lichtenstein, I. Willner, J. Am. Chem. Soc. 123 (2001) 5194–5205.
[4] F. Patolsky, A. Lichtenstein, I. Willner, Angew. Chem. Int. Ed. 39 (2000) 940–943.
[5] J. Wang, A.N. Kawde, M.R. Jan, Biosens. Bioelectron. 20 (2004) 995–1000.
[6] J. Wang, G.D. Liu, M.R. Jan, J. Am. Chem. Soc. 126 (2004) 3010–3011.
[7] H.D. Hill, C.A. Mirkin, Nat. Protocols 1 (2006) 324–336.
[8] F. Patolsky, K.T. Ranjit, A. Lichtenstein, I. Willner, Chem. Commun. 12 (2000) 1025–1026.
[9] I. Willner, F. Patolsky, J. Wasserman, Angew. Chem. Int. Ed. 40 (2001) 1861–1864.
[10] F. Lucarelli, G. Marrazza, M. Mascini, Langmuir 22 (2006) 4305–4309.
[11] R.Q. Thompson, G.C. Barone, H.B. Halsall, W.R. Heineman, Anal. Biochem. 192 (1991) 90–95.
[12] M. Santandreu, F. Céspedes, S. Alegret, E. Martínez-Fàbregas, Anal. Chem. 69 (1997) 2080–2085.
[13] E. Kim, K. Kim, H. Yang, Y.T. Kim, J. Kwak, Anal. Chem. 75 (2003) 5665–5672.
[14] C.G. Bauer, A.V. Eremenko, E. Ehrentreich-Fo1 rster, F.F. Bier, A. Makower, H.B. Halsall, W.R. Heineman, F.W. Scheller, Anal. Chem. 68 (1996) 2453–2458.
[15] J. Das, K. Jo, J.W. Lee, H. Yang, Anal. Chem. 79 (2007) 2790–2796.
[16] S.J. Kwon, H. Yang, K. Jo, J. Kwak, Analyst 133 (2008) 1599–1604.
[17] B. Limoges, D. Marchal, F. Mavre, J.M. Saveant, J. Am. Chem. Soc. 130 (2008) 7276–7286.
[18] E. Nebling, T. Grunwald, J. Albers, P. Schafer, R. Hintsche, Anal. Chem. 76 (2004) 689–696.
[19] B. Elsholz, R. Worl, L. Blohm, J. Albers, H. Feucht, T. Grunwald, B. Jurgen, T. Schweder, R. Hintsche, Anal. Chem. 78 (2006) 4794–4802.
[20] M. Rochelet-Dequaire, N. Djellouli, B. Limoges, P. Brossier, Analyst 134 (2009) 349–353.
[21] Y. Mie, K. Kowata, Y. Hirano, O. Niwa, F. Mizutani, Anal. Sci. 24 (2008) 577–582.
[22] B. Limoges, D. Marchal, F. Mavre, J.M. Saveant, J. Am. Chem. Soc. 128 (2006) 6014–6015.
[23] Y.L. Yuan, R. Yuan, Y.Q. Chai, Y. Zhuo, L.J. Bai, Y.H. Liao, Anal. Biochem. 405 (2010) 121–126.
[24] D. Zheng, N. Wang, F.Q. Wang, D.A. Dong, Y.G. Li, X.Q. Yang, L.H. Guo, J. Cheng, Anal. Chim. Acta 508 (2004) 225–231.
[25] T. Selvaraju, J. Das, K. Jo, K. Kwon, C.H. Huh, T.K. Kim, H. Yang, Langmuir 24 (2008) 9883–9888.
[26] J. Das, M.A. Aziz, H. Yang, J. Am. Chem. Soc. 128 (2006) 16022–16023.
[27] J.E. Clarridge, Clin. Microbiol. Rev. 17 (2004) 840–862.
[28] C. Ruan, Y. Li, Talanta 54 (2001) 1095–1103.
[29] B. Serra, M.D. Morales, A.J. Reviejo, E.H. Hall, J.M. Pingarron, Anal. Biochem. 336 (2005) 289–294.
[30] Z.L. He, L.Y. Wu, X.Y. Li, M.W. Fields, J.Z. Zhou, Appl. Environ. Microbiol. 71 (2005) 3753–3760.
[31] F. Neidhardt, H. Umbarger, Chemical composition of *Escherichia coli*, in: F. Neidhardt, et al. (Eds.), *Escherichia coli* and *Salmonella typhimurium*, 2nd ed., vol. I, ASM Press, Washington, DC, 1996, pp. 13–16.